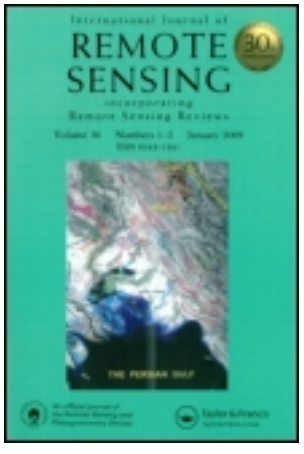

International Journal of Remote Sensing

Publication details, including instructions for authors and subscription information:
http://www.tandfonline.com/loi/tres20

VSDI: a visible and shortwave infrared drought index for monitoring soil and vegetation moisture based on optical remote sensing

Ning Zhang[ab], Yang Hong[b], Qiming Qin[a] & Lu Liu[b]

[a] Institute of Remote Sensing and GIS, Peking University, Beijing, 100871, PR China

[b] School of Civil Engineering and Environmental Sciences, The University of Oklahoma, Norman, OK, 73072, USA

Published online: 26 Mar 2013.

To cite this article: Ning Zhang, Yang Hong, Qiming Qin & Lu Liu (2013) VSDI: a visible and shortwave infrared drought index for monitoring soil and vegetation moisture based on optical remote sensing, International Journal of Remote Sensing, 34:13, 4585-4609, DOI: 10.1080/01431161.2013.779046

To link to this article: http://dx.doi.org/10.1080/01431161.2013.779046

International Journal of Remote Sensing, 2013
Vol. 34, No. 13, 4585–4609, http://dx.doi.org/10.1080/01431161.2013.779046

VSDI: a visible and shortwave infrared drought index for monitoring soil and vegetation moisture based on optical remote sensing

Ning Zhang[a,b], Yang Hong[b], Qiming Qin[a]*, and Lu Liu[b]

[a]*Institute of Remote Sensing and GIS, Peking University, Beijing 100871, PR China;* [b]*School of Civil Engineering and Environmental Sciences, The University of Oklahoma, Norman, OK 73072, USA*

(*Received 13 June 2012; accepted 19 October 2012*)

In this article, a new index, the visible and shortwave infrared drought index (VSDI), is proposed for monitoring both soil and vegetation moisture using optical spectral bands. VSDI is defined as $\mathrm{VSDI} = 1 - [(\rho_{\mathrm{SWIR}} - \rho_{\mathrm{blue}}) + (\rho_{\mathrm{red}} - \rho_{\mathrm{blue}})]$, where ρ represents the reflectance of shortwave infrared (SWIR) red and blue channels, respectively. VSDI is theoretically based on the difference between moisture-sensitive bands (SWIR and red) and moisture reference band (blue), and is expected to be efficient for agricultural drought monitoring over different land-cover types during the plant-growing season. The fractional water index (FWI) derived from 49 Mesonet stations over nine climate divisions (CDs) across Oklahoma are used as ground truth data and VSDI is compared with three other drought indices. The results show that VSDI generally presents the highest correlation with FWI among the four indices, either for whole sites or for individual CDs. The NDVI threshold method is applied to demonstrate the satisfactory performance of VSDI over different land-cover types. A time-lag analysis is also conducted and suggests that VSDI can be used as a real-time drought indicator with a time lag of less than 8 days. The VSDI drought maps are produced and compared with the US Drought Monitor (USDM) maps. A good agreement has been observed between the two products, and finer spatial information is also found in VSDI. In conclusion, VSDI appears to be a real-time drought indicator that is applicable over different land-cover types and is suitable for drought monitoring through the plant-growing season.

1. Introduction

Drought is a slow-onset natural hazard with effects that accumulate over a considerable period of time (weeks to years) (Wardlow, Anderson, and Verdin 2012). It can be classified into three physically based categories: meteorological, agricultural, and hydrological drought (Dracup, Lee, and Paulson 1980; Wilhite 2000). In this article, we focus primarily on agricultural drought, which refers to a period characterized by declining soil moisture and consequent crop failure without any reference to surface water resources (Mishra and Singh 2010). Agricultural drought is generally a short-term dryness (e.g. a few weeks' duration), but occurs at a critical time during the growing season and can severely reduce crop yields (Heim 2002). In the Canadian prairies, the season droughts during 1988 and 2001 each resulted in more than $5 thousand million in agricultural losses (Wheaton et al. 1992; Phillips 2002). In 1995, the US Federal Emergency Management Agency (FEMA)

*Corresponding author. Email: qmqinpku@163.com; qmqin@pku.edu.cn

estimated that US drought events caused a loss of $6–8 thousand million on average each year (FEMA 1995).

Satellite remote sensing is an effective way to monitor drought, considering its large spatial coverage and relatively high temporal and spatial resolution. Numerous satellite-based methods have been developed to describe land-surface moisture conditions. Gutman (1990) gave an overview of drought monitoring methods using the first generation of remote sensing satellites, and this was followed by an update by Kogan (1997). Recent reviews were provided by Niemeyer (2008) that summarized the then latest drought indices from different disciplines, Wang and Qu (2009) presented a review on soil moisture monitoring based on remote sensing, and Zhang et al. (2010) reviewed vegetation moisture monitoring using optical remote sensing.

Optical remote sensing with wavelengths between 0.4 and 2.5 μm has commonly been used in operational drought monitoring (McVicar and Jupp 1998; Kogan 2000; Heim 2002; Zhang et al. 2010), as in the vegetation drought response index (VegDRI) (Brown et al. 2008) and the US Drought Monitor (USDM) (Svoboda et al. 2002). Drought indices based on optical remote sensing can generally be classified into three categories by their targets: one is for soil moisture monitoring, the second is on vegetation drought monitoring, and the third is for both soil and vegetation moisture monitoring.

For vegetation drought monitoring with optical remote sensing, the normalized difference vegetation index (NDVI) is the most extensively applied vegetation index, which uses the normalized difference between near-infrared (NIR) and red reflectance (McVicar and Bierwirth 2001; Ji and Peters 2003; Wan, Wang, and Li 2004; Wang et al. 2007; Gu et al. 2007, 2008; Brown et al. 2008). NDVI-based indices such as the anomaly vegetation index (AVI) (Chen, Xiao, and Sheng 1994; Anyamba, Tucker, and Eastman 2001) and the vegetation condition index (VCI) (Kogan 1990, 1995) were also developed to normalize vegetation seasonal variation and better characterize drought patterns. The application of NDVI and NDVI-based methods for drought monitoring is made under the assumption that water stress is the only factor that interferes with the plant-growing process. However, in the real world other factors such as insects, wild fires, and pollution may also interrupt plants' normal growth and add uncertainties to drought interpretation. Besides, the time lag between the occurrence of drought and NDVI response (Di, Rundquist, and Han 1994; Wang, Price, and Rich 2001; Adegoke, and Carleton 2002; Wang et al. 2007) makes NDVI and NDVI-based indices unsuitable for real-time drought monitoring (Ghulam et al. 2007b).

By using a combination of NIR and shortwave infrared (SWIR) bands, a new set of vegetation drought indices are proposed as an advanced and direct vegetation moisture indicator over NDVI, including the leaf water content index (LWCI; Hunt, Rock, and Nobel 1987), the normalized difference infrared index (NDII; Hardisky, Klemas, and Smart 1983), the global vegetation moisture index (GVMI; Ceccato et al. 2002), and the SWIR perpendicular water stress index (SPSI; Ghulam et al. 2007a). Among the above indices, NDII is the most popular and has been studied and referred to under different names. Hardisky, Klemas, Smart (1983) proposed NDII with the equation $\mathrm{NDII} = \rho_{850} - \rho_{1650} \big/ \rho_{850} + \rho_{1650}$ to estimate canopy water content; Gao (1996) developed the normalized difference water index (NDWI) to quantify vegetation moisture with NIR reflectance at 860 and 1240 nm as $\mathrm{NDWI} = (\rho_{860} - \rho_{1240})/(\rho_{860} + \rho_{1240})$; Fensholt and Sandholt (2003) adopted MODIS band 2 (NIR) and band 5 or 6 (SWIR) reflectance to calculate the shortwave infrared water stress index (SIWSI) in $\mathrm{SIWSI}(5/6, 2) = (\rho_{\mathrm{SWIR5/6}} - \rho_{\mathrm{NIR2}})/(\rho_{\mathrm{SWIR5/6}} + \rho_{\mathrm{NIR2}})$; Xiao et al. (2004a, 2004b) used the NIR and the MIR bands for SPOT-4 VEGETATION data and bands 2 and 6 for MODIS data in NDII, and defined this as the land surface water index

(LSWI) in the form LSWI $= (\rho_{NIR} - \rho_{SWIR})/(\rho_{NIR} + \rho_{SWIR})$. Despite variation in specific wavelengths or sensor-dependent bands used to calculate NDII, one thing in common is that the NIR band serves as a moisture reference band and the SWIR band is used as the moisture-measuring band. All the above indices have proved to be effective in monitoring vegetation water content in a variety of studies (Hunt and Rock 1989; Zarco-Tejada, Rueda, and Ustin 2003; Jackson et al. 2004; Maki, Ishiahra, and Tamura 2004; Chen, Huang, and Jackson 2005; Zhao et al. 2009), whereas uncertainties are considerably increased in the presence of soil. In other words, vegetation drought indices are more applicable over moderate to densely vegetated surfaces, but not over sparsely vegetated or bare soil surfaces, because soil effects are not considered during their calculation (Gao 1996; Ghulam et al. 2007a, 2008a).

For soil moisture monitoring, Ghulam, Qin, and Zhan (2006) designed the perpendicular drought index (PDI) based on the NIR-Red spectral reflectance space. PDI is quite efficient over bare soil surfaces, but it does not perform well over vegetated areas (Ghulam et al. 2008b; Qin et al. 2008). To solve this problem, Ghulam et al. (2007b) introduced the vegetation fraction into PDI and proposed the modified perpendicular drought index (MPDI), which is capable of measuring water content over differing land surfaces from bare soil to moderately vegetated areas. However, the operational application of PDI and MPDI are still challenged by their assumption of an invariant soil line, which in fact varies with soil type, soil fertility, and land topography. In addition, the determination of the soil line is also user dependent to some extent. To avoid these uncertainties, the distance drought index (DDI; Yang et al. 2008) was developed based on the NIR-Red spectral space. This index is also applicable in the presence of vegetation, which is an improvement on PDI and, more importantly, it is independent of the fixed soil line (Qin et al. 2010). The assumption regarding the full range of soil moisture variation, however, may limit the application of DDI. By using the normalized difference between MODIS bands 6 and 7, Du et al. (2007) proposed the surface water capacity index (SWCI) specialized for surface soil moisture monitoring using MODIS data. This index has proved to be highly correlated with soil moisture at the 0–50 cm layer (Zhang et al. 2008). Compared with vegetation water indices, soil moisture indices may have a more direct and rapid response to water deficiency because plants have an ability to resist drought that may cause a delay in the identification of drought occurrence. However, soil moisture indices are not as efficient as vegetation moisture indices when applied over densely vegetated surface or the full vegetation area, which may limit their application over large areas to some extent.

Compared with the first two categories, fewer approaches are proposed for both soil and vegetation moisture monitoring using optical remote sensing. Wang and Qu (2007) proposed the normalized multi-band drought index (NMDI) to estimate water content for both soil and vegetation surface. However, this index has inconsistent relationships with soil and vegetation moisture changes. Specifically, it has a positive correlation with vegetation water variation while exhibiting a negative correlation with soil moisture changes. Therefore, when applied to areas with moderate vegetation coverage, considerable uncertainty will occur, and the roles of NMDI as soil drought indicator and vegetation drought indicator may blur and result in inaccurate results (Wang and Qu 2007). An alternate approach, the N-dimensional dryness index (NDDI) (Ghulam et al. 2011), was recently designed to quantify soil moisture in various canopy coverage conditions based on N-dimensional spectral space. Many variables are used in this index, including land-surface temperature, vegetation index, albedo, and other bio/geophysical parameters that may indicate the soil moisture condition. It is important to consider as many variables as possible to accurately

characterize drought status, but simultaneous utilization of multiple variables may hinder operational drought monitoring if the required variables are not available concomitantly.

In conclusion, a simple, stable, and operational drought indicator that is robust for both soil and vegetation cover is still worth exploring. This is especially true for agricultural drought monitoring over large areas or throughout the plant-growing season, where land-cover types may change from place to place and vegetation coverage may vary temporally. In these cases, neither vegetation moisture indices nor soil moisture indices (SWCI) may work well in isolation, due to their restricted fields of application. One possible solution may be to perform land-cover classification and assign a suitable index for each class, while another could be to apply different moisture indices at different plant-growing stages. The classification accuracy and the combined use of different drought indices may add additional uncertainty to the final results and also add to the complexity of agricultural drought monitoring.

The objective of this study was to explore the potential of using multi-spectral bands in the optical domain to quantify surface moisture for both soil and vegetation covers and to provide an operational solution for agricultural drought monitoring over different land covers or throughout the plant-growing season.

2. Development of VSDI

2.1. Spectral response to water stress for plants and soil

Vegetation spectral response to water stress has been reported in many studies on different plants, including spinach (Aldakheel and Danson 1997), snapbean (Ripple 1986), soybean (Yu et al. 2000), maize (Zygielbaum et al. 2009), and other species of trees, crops, and plants (Carter 1991, 1993; Ceccato et al. 2001). All the above studies have reported an overall increase in plant reflectance from 0.4 to 0.25 μm when plants are water stressed. Figure 1 shows an example of laboratory-measured reflectance spectra (Elvidge 1990) for fresh and dry redwood leaf. The physiological features of different spectra are also illustrated in Figure 1.

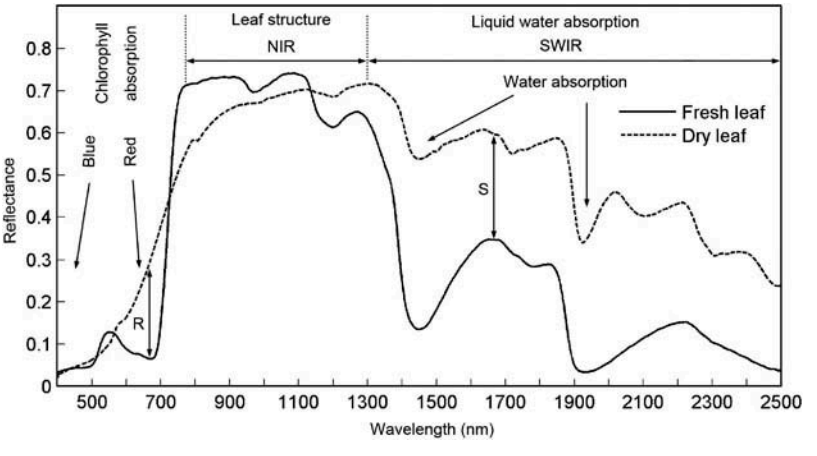

Figure 1. Examples of laboratory-measured fresh and dry vegetation (redwood) reflectance spectra measured by Elvidge (1990); 'R' and 'S', respectively, indicate the increased reflectance between fresh and dried redwood leaf in the red and SWIR spectra.

Note: The dominant physiological features for different spectra are also labelled in this figure.

As we can see from Figure 1, with reduced plant water there is an obvious increase in plant reflectance in the red and SWIR spectrum. A variable pattern of NIR reflectance can also be observed, but reflectance in the blue spectrum shows an insignificant change. This is generally consistent with previous studies (mentioned above). Spectral variation at different wavelengths can be explained by the following.

In regard to the visible spectrum (0.4–0.74 μm), healthy plant reflectance is mainly governed by pigments, especially the blue (0.4–0.52 μm) and red (0.63–0.69 μm) regions (Ollinger 2011), where two spectral valleys caused by the strong absorption of chlorophyll are found (Figure 1). If a plant is subject to water stress that interrupts its normal growth, its chlorophyll production may be decreased or terminated, which results in reduced chlorophyll absorption in the blue and red bands (Lillesand, Kiefer, and Chipman 2008), with increased reflectance observed in the visible spectrum (Carter 1991). In particular, the red spectrum is more sensitive to water stress than the blue (Jensen 2007), which results in more significant reflectance change in the red spectrum (indicated as the distance '*R*' in Figure 1) than in the blue.

Reflectance in the NIR spectrum (0.74–1.3 μm) is most sensitive to leaf internal structure changes (Ripple 1986; Jacquemoud and Baret 1990; Jacquemoud et al. 1995) and is unresponsive to moisture variations compared with other spectral regions (Elvidge and Lyon 1985; Carter 1993; Chuvieco et al. 2002). Only when stress has developed sufficiently to cause severe leaf dehydration (which dramatically changes the leaf's mesophyll structure) will an obvious increase in NIR spectral reflectance be presented (Jensen 2007). Furthermore, NIR plant reflectance is also greatly affected by leaf area index (LAI), plant type, and plant density (Elachi 1987; Jacquemoud 1993; Ceccato et al. 2001). In other words, the NIR reflectance of plants is indirectly affected by water stress, and its variation is a combined reflection of multiple factors. This might explain the fluctuation in NIR reflectance as shown in Figure 1.

For the SWIR (1.3–2.5 μm) spectrum, many studies (Hunt and Rock 1989; Zarco-Tejada, Rueda, and Ustin 2003; Ghulam et al. 2008a) have proved that it has a strong relationship with leaf water variation and this band is more sensitive to moisture variation than the visible or NIR spectrum (Dawson et al. 1999; Ceccato et al. 2001; Chuvieco et al. 2002). This explains the significant reflectance increase at the SWIR spectrum as indicated by the distance 'S' in Figure 1.

Based on the above analysis, SWIR is the most sensitive spectrum to vegetation water variation, followed by the red. The blue can be viewed as the band least sensitive to vegetation moisture variation compared with the other bands. In this way, the difference between the water-sensitive band (SWIR and red) and the less sensitive band (blue) can be used to maximize moisture variation and reduce the influence of leaf structure, which has an overall effect through the whole optical wavelength (Aldakheel and Danson 1997; Yu et al. 2000; Zygielbaum et al. 2009) at the same time.

In regard to spectral response to soil moisture changes, previous research has proved that the whole spectrum of soil reflectance will diminish with increase in soil moisture at low moisture stages (Bowers and Hanks 1965; Lobell and Asner 2002; Liu et al. 2002, 2003; Bach and Verhoef 2003; Whiting et al. 2004). Although soil reflectance is also influenced by other factors, such as soil texture, mineral composition, and organic matter (Bowers and Hanks 1965; Baumgardner et al. 1985), these factors can be considered as unchanged with time for a given location, and thus soil reflectance is primarily determined by soil moisture (Liu et al. 2002). Figure 2 shows soil reflectance curves measured by Whiting et al. (2004) using a low-sodicity soil sample from Lemoore, USA at different oven-dried water contents (0.03, 0.12, 0.20, 0.30, and 0.42 g g^{-1}).

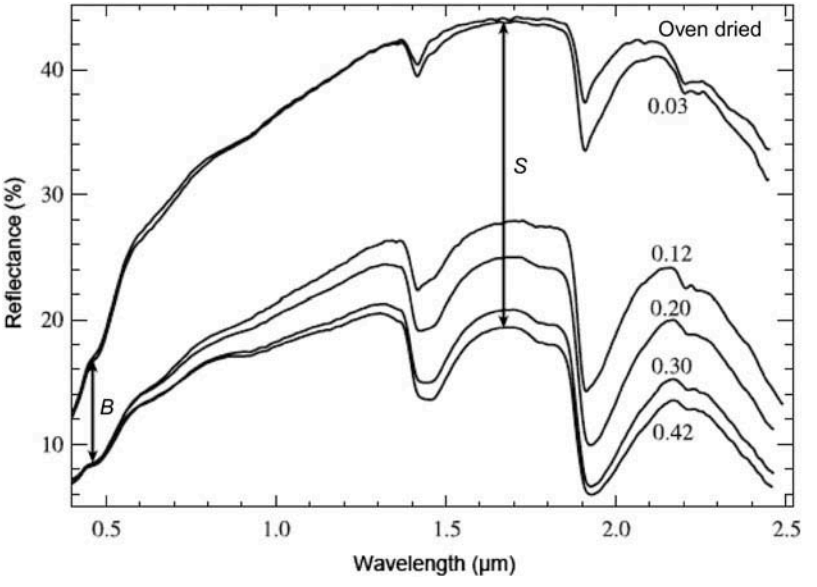

Figure 2. Soil reflectance with varying oven-dried gravimetric water content (0.03, 0.12, 0.20, 0.30, and 0.42 g g^{-1}), modified after Whiting et al. (2004).

Note: '*B*' denotes variation of soil reflectance in the blue spectrum when water stressed, and '*S*' denotes variation of soil reflectance in the SWIR spectrum when water stressed.

In Figure 2, reflectance increase can be observed throughout the whole spectrum of soil with decreased soil moisture. In addition, increased reflectance is also reinforced at longer wavelengths, which indicates that spectral sensitivity to soil moisture is enhanced with increase in wavelength. In this case, the blue spectral region (0.4–0.52 μm), which presents the smallest *y*-axis increment (indicated by distance '*B*' in Figure 2), is least sensitive to soil water variation, whereas the SWIR spectrum (1.3–2.5 μm), which presents the largest increment in the *y*-axis (indicated by distance '*S*' in Figure 2), is most sensitive to soil moisture changes.

When comparing spectral response between soil and vegetation when water stressed, a common feature is that decrease in water content is connected to an increase in reflectance over the optical wavelength range (0.4–2.5 μm), especially for the red and SWIR spectrum. In general, with increasing wavelength, reflectance response is also intensified. Taking advantage of this common feature, it is possible to use the difference between channels of different water sensitivity to estimate water content over different land-cover types. This is the theoretical basis for the visible and shortwave infrared drought index (VSDI) described below.

2.2. *The formation of VSDI*

The VSDI is proposed here to monitor moisture variation for both soil and vegetation. It is developed by using the differences among the three bands located in the blue and red and SWIR spectra, and is defined as

$$\mathrm{VSDI} = 1 - [(\rho_{\mathrm{SWIR}} - \rho_{\mathrm{blue}}) + (\rho_{\mathrm{red}} - \rho_{\mathrm{blue}})], \quad (1)$$

where, ρ_{SWIR}, ρ_{blue}, and ρ_{red} are the reflectances of SWIR, blue, and red bands, respectively. Based on the above analysis, the SWIR and red channels are both sensitive to water variation for soil and vegetation, and the blue channel is less sensitive to moisture changes for both. Therefore, the SWIR and red bands can serve as the moisture-measuring channel in VSDI, while the blue band is used as the reference channel or the benchmark for moisture variation. The combination of the difference between SWIR and blue ($\rho_{SWIR} - \rho_{blue}$) and the difference between red and blue ($\rho_{red} - \rho_{blue}$) may maximize moisture variation and have the potential to estimate surface water independent of land-cover types. Finally, the entire item $(\rho_{SWIR} - \rho_{blue}) + (\rho_{red} - \rho_{blue})$ is subtracted from 1 to make VSDI positively correlated to moisture variation. The ideal VSDI range is defined in Table 1 with a brief explanation.

As defined in Table 1, the overall range of VSDI is above zero, and the larger the value the wetter the condition indicated. In this study, land surface can be simplified into four types: soil, vegetation, a combination of the two, and water. For the first three types, VSDI is within the range between 0 (dry) and 1 (wet) and has a consistently positive correlation with moisture variation. This is, intuitively, an advantage over NMDI, which shows an opposite correlation with water variation in terms of soil and vegetation. For water surfaces (water and snow water equivalent, including snow and ice cover), the blue reflectance of which is higher than for red and SWIR, the VSDI value is larger than 1. Since water and snow can be deemed as an extreme case of wet conditions, this is still in agreement with the moisture-monitoring ability of VSDI. Using the above definition, the use of VSDI can be anticipated as a drought index applicable over different land-cover types (the four simplified types).

It is also worth explaining that the NIR channel was not considered in our study for two reasons. First, as mentioned above, NIR reflectance does not have a direct response to water stress and is readily affected by many factors (leaf structure, LAI, plant density, and plant type), and thus cannot be used as a water-sensitive (or water-measuring) band in VSDI. Second, NIR is not used as the moisture reference band because it varies greatly among different land-cover types, especially soil and vegetation. For example, the NIR reflectance of a healthy plant is much higher than that of bare soil. If NIR is used as the reference band, the benchmark of plant moisture variation will be much higher than that of soil, which will make VSDI incomparable among different land-cover types. In other words, land-cover type-induced variation will overwhelm moisture-induced variation when NIR is used as the reference band. In contrast, the blue spectrum remains at a consistently low value for both vegetation and soil and is least sensitive for vegetation and soil moisture variation (Figures 1 and 2) compared with NIR, and thus it is preferable to NIR as the reference band in the construction of VSDI.

In the application of the VSDI, the 1.5–1.8 μm SWIR domain is suggested as the SWIR channel in VSDI. This is because with increased wavelength, solar radiation is reduced but contamination from atmospheric water vapour is worsened (Roberts, Green, and Adams

Table 1. The definition of ideal VSDI range.

$0 < \text{VSDI} \leq 1$	The larger the value, the wetter the conditions indicated (for surfaces on farmland or any surface that can be simplified as soil, vegetation, or a combination of the two)
$\text{VSDI} > 1$	Water or snow water equivalent (including water body, snow, and ice cover)

1997; Sims and Gamon 2003). Therefore, the water measurement band selected in the shorter regions of the SWIR domain or the longer wavelengths of the NIR domain may provide more accurate moisture information (Tucker 1980; Jackson, Slater, and Pinter 1983; Sims and Gamon 2003; Ghulam et al. 2008a). Ghulam et al. (2007a) has proved that the TM/ETM+ band 5 (1.55–1.75 μm) has a stronger correlation with leaf water content than band 7 (2.08–2.35 μm). Zhao et al. (2009) also suggested that the SIWSI index calculated using MODIS band 6 (1.63–1.65 μm) yielded better moisture estimation than band 7 (2.11–2.16 nm). Therefore, considering different remote sensors, the use of band 5 for Landsat data and band 6 for MODIS data is suggested as the SWIR band when calculating VSDI.

3. Validation

3.1. *Test sites and validation data*

Our study area is located in Oklahoma, which lies in the South Central region of the USA. As a drought-prone region, Oklahoma is an ideal location for new drought index testing and validation. In 2011, Oklahoma suffered an exceptional drought, the state-wide average precipitation from January to October reaching about 13 inches below normal (OCS Monthly Climate Summaries, http://climate.ok.gov/index.php/climate/summary/reports_summaries). Therefore, the validation period selected in this study was 6 March to 8 November 2011. Oklahoma climatology varies significantly across the state, with temperatures increasing from north to south (Figure 3(*a*)) and precipitation increasing from west to east (Figure 3(*b*)). Therefore, nine climate divisions (CDs) for Oklahoma (Figure 3) were used in this study to compare drought indices, considering that weather and climate patterns are homogeneously distributed in the same CD.

An extensive environmental observation network is well established and distributed over Oklahoma, known as the Oklahoma Mesonet (Brock et al. 1995). The Oklahoma Mesonet consists of 120 automated stations with at least one in each of Oklahoma's 77 counties. This network provides quality-controlled measurements of meteorological and land-surface parameters such as precipitation, temperature, and soil moisture every 5 min (http://www.mesonet.org/). The soil moisture instruments installed in Mesonet stations are 229-L heat-dissipation sensors, by which soil moisture variation is recorded in the form of temperature difference (ΔT). In this case, the fractional water index (FWI) (Schneider et al. 2003) specialized for the heat-dissipation sensor is used to quantify *in situ* soil moisture.

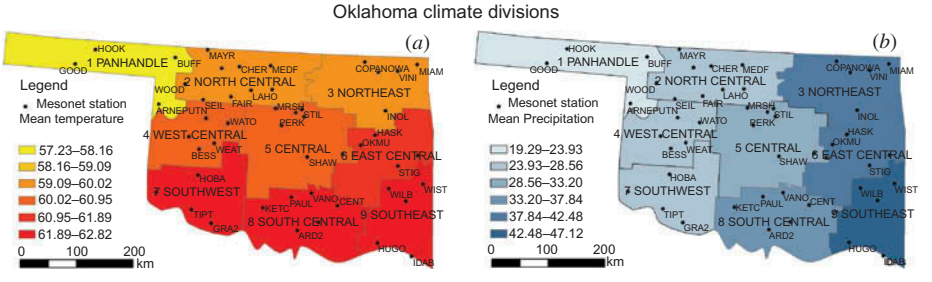

Figure 3. Mean temperature (Figure 3(*a*)) and mean precipitation (Figure 3(*b*)) over 30 years (1971–2000) for the nine climate divisions (CDs) of Oklahoma.

Note: The climate data were obtained from the US Geological Survey (USGS) website (http://water.usgs.gov/GIS/metadata/usgswrd/XML/climate_div.xml).

FWI is a relative measure of soil wetness and is independent of soil texture at each site, and is thus comparable among different Mesonet stations. FWI can be calculated using Equation (2),

$$\mathrm{FWI} = (\Delta T_{\mathrm{d}} - \Delta T_{\mathrm{sensor}})/(\Delta T_{\mathrm{d}} - \Delta T_{\mathrm{w}}), \tag{2}$$

where $\Delta T_{\mathrm{sensor}}$ represents sensor-measured temperature difference (°C), ΔT_{d} is the sensor response constant (3.96°C) in dry conditions, and ΔT_{w} is the sensor response constant (1.38°C) in wet conditions. The value of FWI ranges from 0 (very dry soil) to 1 (purely saturated soil). Considering the high level of noise for soil moisture at 5 cm due to its sensitivity to environmental change, and the imperceptibility of optical remote sensing signals at 60 cm or deeper, only daily FWI at 25 cm was calculated and used as ground truth data for soil moisture.

In this study, four criteria were applied to select the validation sites from the 120 Mesonet stations. (1) The validation sites should be evenly distributed within the nine CDs. In this way, 4–9 stations were selected from each CD. (2) A continuous soil moisture measurement should be available for the selected stations during our validation period. The time gap for the 25 cm FWI data on the selected sites was under 1 month. (3) Stations located in sandy areas should be excluded since the 229-L heat dissipation sensors installed in Mesonet stations do not perform well in sandy soils (Schneider et al. 2003). In this sense, the sand percentage of the selected sites at the 25 cm layer was less than 50%. (4) The selected stations should be located in plant-growing areas, and sites located within urban areas to be excluded for the purpose of examining the applicability of a drought index throughout the plant-growing season. The cropland data layer (CDL) was used to identify the land cover for each site in Oklahoma (Figure 4). CDL is a geo-referenced, crop-specific land-cover classification product released by the National Agricultural Statistics Service (NASS) (Johnson and Mueller 2010) and accessible from the Geospatial Data Gateway at http://datagateway.nrcs.usda.gov/. The 2011 CDL of Oklahoma has a high spatial resolution

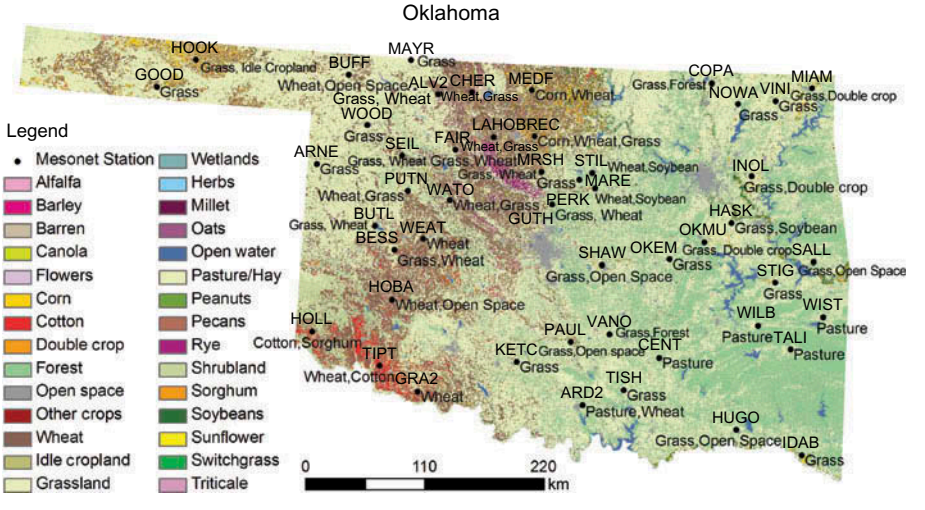

Figure 4. Locations and names of the 49 Oklahoma Mesonet stations; the land-cover type for each site was identified from the 2011 cropland data layer (CDL) of the National Agricultural Statistics Service (NASS) (Johnson and Mueller 2010).

of 30 m and an overall accuracy of 82.9% (http://www.nass.usda.gov/research/Cropland/metadata/metadata_ok11.htm). These criteria were strictly applied to site selection, and finally 49 Mesonet stations were selected from 120, indicated by black dots in Figures 3 and 4. The land-cover type for each site is also labelled in Figure 4 and Table 2.

To be consistent with the temporal sample of MODIS products, daily 25 cm FWI for the selected 49 sites was averaged every 8 days, and the data gap linearly interpolated by nearby dates. The Savitzky–Golay approach (Savitzky and Golay1964; Gorry 1990) with a polynomial order of 1 and a window size of 3 was then applied to the complete 8 day FWI data set to reduce additional turbulence and noise.

The remote sensing data used in this study were MODIS 8 day surface reflectance products (MOD09A1) collected from http://ladsweb.nascom.nasa.gov/data. The spatial resolution of MOD09A1 is 500 m for bands 1–7 covering the visible, NIR, and SWIR spectral domains. Two tiles covering Oklahoma (h10v05 and h09v05) were mosaicked and the MODIS time-series data (a total of 31 images) was produced during our validation period (6 March to 8 November 2011). A quality control process was applied to filter the 'cloud' and 'high-aerosol' pixels identified from the MODIS quality assurance data product. To reduce additional atmospheric noise, the MODIS time-series data were also smoothed using the Savitzky–Golay filter (polynomial order 1, window size 3). The time series of VSDI, LSWI, SWCI, and NMDI data were then calculated for the 500 m pixel that geographically corresponded to each study site. It is also assumed in this study that the field measurements at each station represent a MODIS pixel with an average value of 500 × 500 m. The equations for LSWI, SWCI, and NMDI based on MODIS data are as follows:

$$\mathrm{LSWI} = \frac{\rho_{\mathrm{NIR}} - \rho_{\mathrm{SWIR6}}}{\rho_{\mathrm{NIR}} + \rho_{\mathrm{SWIR6}}}, \tag{3}$$

$$\mathrm{SWCI} = \frac{\rho_{\mathrm{SWIR6}} - \rho_{\mathrm{SWIR7}}}{\rho_{\mathrm{SWIR6}} + \rho_{\mathrm{SWIR7}}}, \tag{4}$$

$$\mathrm{NMDI} = \frac{\rho_{\mathrm{NIR}} - (\rho_{\mathrm{SWIR6}} - \rho_{\mathrm{SWIR7}})}{\rho_{\mathrm{NIR}} + (\rho_{\mathrm{SWIR6}} - \rho_{\mathrm{SWIR7}})}, \tag{5}$$

where ρ_{NIR}, ρ_{SWIR6}, ρ_{SWIR7} are, respectively, the reflectance for the MODIS NIR and SWIR regions at bands 6 and 7.

3.2. *Correlation coefficient (r) analysis*

To validate the performance and reliability of VSDI, it was necessary to compare it with ground measurements and other widely used drought indices. For this purpose, a 25 cm FWI was used as ground truth soil moisture, and one commonly used vegetation drought index (LSWI), one SWCI, and one drought indicator for both soil and vegetation moisture (NMDI) were selected for comparison with VSDI.

3.2.1. *Comparison among sites and CDs*

The correlation coefficient (r) was first calculated between the four drought indices and the 25 cm FWI over 49 sites and nine CDs. Figure 5 shows the scatter plot for the four indices with the statistics from 49 Mesonet stations (1519 samples, 49 sites × 31 periods/site).

Table 2. Correlation analysis between four drought indices (VSDI, LSWI, SWCI, and NMDI) and 25 cm FWI from 6 March to 8 November for 49 sites over nine climate divisions in Oklahoma.

			VSDI		LSWI		SWCI		NMDI		VSDI-CD		LSWI-CD		SWCI-CD		NMDI-CD	
Climate division	Land-cover type	Station ID	*R*	*p*-value	*r*	*p*-value	*r*	*p*-value	*r*	*p*-value	*r*	*p*-value	*r*	*p*-value	*r*	*p*-value	*r*	*p*-value
1 Panhandle	Grass	GOOD	0.84	0.000	−0.48	0.006	**0.13**	**0.481**	**−0.22**	**0.236**	0.41	0.000	**0.06**	**0.522**	0.28	0.002	−0.32	0.000
	Grass, Idle land	HOOK	**0.25**	**0.174**	**−0.25**	**0.183**	0.60	0.000	−0.63	0.000								
	Grass	ARNE	0.75	0.000	−0.63	0.000	**−0.12**	**0.537**	−0.47	0.007								
	Wheat, Open space	BUFF	0.65	0.000	0.88	0.000	0.88	0.000	−0.87	0.000								
2 North central	Grass	WOOD	0.47	0.007	**0.11**	**0.546**	0.42	0.019	−0.54	0.002	0.58	0.000	0.37	0.000	0.44	0.000	−0.17	0.003
	Grass, Wheat	SEIL	0.49	0.005	**0.07**	**0.709**	**0.07**	**0.719**	**0.04**	**0.817**								
	Grass	MAYR	0.73	0.000	**0.05**	**0.769**	0.47	0.007	−0.57	0.001								
	Grass, Wheat	ALV2	0.90	0.000	0.68	0.000	0.79	0.000	−0.61	0.000								
	Grass, Wheat	FAIR	0.82	0.000	0.56	0.001	0.36	0.048	**−0.16**	**0.376**								
	Wheat, Grass	CHER	0.64	0.000	0.68	0.000	0.50	0.004	**−0.21**	**0.249**								
	Wheat, Grass	LAHO	0.80	0.000	0.66	0.000	0.80	0.000	−0.69	0.000								
	Corn, Wheat	MEDF	0.83	0.000	0.55	0.001	**0.33**	**0.070**	**0.34**	**0.059**								
	Corn, Wheat, Grass	BREC	0.79	0.000	0.72	0.000	0.56	0.001	**−0.05**	**0.789**								
3 Northeast	Grass, Forest	COPA	**0.35**	**0.057**	**0.07**	**0.714**	**0.08**	**0.679**	**0.09**	**0.636**	0.41	0.000	0.28	0.000	0.24	0.002	0.28	0.000
	Grass	NOWA	0.49	0.005	**0.29**	**0.108**	**0.36**	**0.050**	**0.22**	**0.245**								
	Grass, Double crop	INOL	0.55	0.001	**0.33**	**0.070**	**0.21**	**0.250**	0.44	0.012								
	Grass	VINI	0.49	0.005	0.54	0.002	**0.35**	**0.051**	0.67	0.000								
	Grass, Double crop	MIAM	0.43	0.016	**0.27**	**0.136**	**0.19**	**0.305**	**0.28**	**0.127**								
4 West central	Grass, Wheat	BUTL	0.67	0.000	−0.53	0.002	0.82	0.000	−0.82	0.000	0.69	0.000	0.36	0.000	0.53	0.000	−0.34	0.000
	Grass, Wheat	BESS	0.83	0.000	**−0.30**	**0.096**	0.47	0.007	−0.66	0.000								
	Wheat, Grass	PUTN	0.80	0.000	0.78	0.000	0.65	0.000	−0.38	0.034								
	Wheat	WEAT	0.76	0.000	0.75	0.000	0.78	0.000	−0.73	0.000								
	Wheat, Grass	WATO	0.74	0.000	0.45	0.012	0.42	0.019	**−0.12**	**0.519**								
5 Central	Grass, Wheat	MRSH	0.81	0.000	0.61	0.000	0.68	0.000	−0.46	0.010	0.45	0.000	0.37	0.000	0.19	0.005	0.14	0.033
	Grass, Wheat	GUTH	0.70	0.000	0.81	0.000	0.80	0.000	−0.62	0.000								
	Grass	MARE	**0.28**	**0.129**	**0.04**	**0.824**	**0.01**	**0.970**	**0.11**	**0.547**								
	Wheat, Soybean	STIL	0.75	0.000	0.54	0.002	**0.34**	**0.058**	0.56	0.001								
	Wheat, Soybean	PERK	0.62	0.000	0.54	0.002	**0.33**	**0.074**	**0.16**	**0.393**								
	Grass, Open space	SHAW	0.55	0.001	**0.21**	**0.253**	0.36	0.047	**0.04**	**0.824**								
	Grass	OKEM	0.64	0.000	0.67	0.000	0.67	0.000	0.61	0.000								
6 East Central	Grass, Double crop	OKMU	**0.34**	**0.061**	**0.34**	**0.059**	**0.21**	**0.247**	0.43	0.015	0.35	0.000	0.31	0.000	**0.16**	**0.070**	0.42	0.000
	Grass, Soybean	HASK	0.48	0.006	**0.22**	**0.233**	**0.15**	**0.417**	**0.35**	**0.054**								
	Grass	STIG	0.63	0.000	0.55	0.001	0.38	0.037	0.71	0.000								

(*Continued*)

Table 2. (*Continued*).

			VSDI		LSWI		SWCI		NMDI		VSDI-CD		LSWI-CD		SWCI-CD		NMDI-CD	
Climate division	Land-cover type	Station ID	*R*	*p*-value	*r*	*p*-value	*r*	*p*-value	*r*	*p*-value	*r*	*p*-value	*r*	*p*-value	*r*	*p*-value	*r*	*p*-value
	Grass, Open space	SALL	0.50	0.004	**0.31**	**0.095**	**0.09**	**0.629**	0.45	0.012								
7 Southwest	Cotton, Sorghum	HOLL	0.37	0.042	−0.51	0.003	**−0.04**	**0.843**	**−0.17**	**0.348**	0.48	0.000	0.34	0.000	0.38	0.000	−0.24	0.008
	Wheat, Cotton	TIPT	0.51	0.003	0.55	0.001	0.49	0.006	**−0.18**	**0.343**								
	Wheat, Open space	HOBA	0.59	0.001	**0.33**	**0.066**	**−0.18**	**0.329**	0.42	0.017								
	Wheat	GRA2	0.53	0.002	0.58	0.001	0.59	0.000	**−0.27**	**0.147**								
8 South Central	Grass	KETC	0.54	0.002	**−0.11**	**0.562**	**0.27**	**0.148**	−0.44	0.014	0.50	0.000	0.25	0.001	0.26	0.000	0.17	0.018
	Grass, Open space	PAUL	0.72	0.000	**0.11**	**0.565**	**0.24**	**0.187**	**−0.03**	**0.859**								
	Pasture, Wheat	ARD2	0.77	0.000	**0.29**	**0.107**	**0.25**	**0.172**	**0.33**	**0.074**								
	Grass, Forest	VANO	0.40	0.026	**−0.04**	**0.835**	**−0.05**	**0.807**	**0.02**	**0.923**								
	Grass	TISH	0.76	0.000	0.45	0.012	0.53	0.002	**0.32**	**0.075**								
	Pasture	CENT	0.61	0.000	0.37	0.041	**0.29**	**0.112**	**0.34**	**0.064**								
9 Southeast	Grass, Open space	HUGO	0.77	0.000	0.75	0.000	0.70	0.000	0.74	0.000	0.74	0.000	0.64	0.000	0.59	0.000	0.65	0.000
	Pasture	WILB	0.68	0.000	0.56	0.001	0.44	0.013	0.68	0.000								
	Pasture	TALI	0.87	0.000	0.81	0.000	0.81	0.000	0.76	0.000								
	Grass	IDAB	0.67	0.000	0.44	0.013	0.47	0.007	0.36	0.048								
	Pasture	WIST	0.90	0.000	0.70	0.000	0.67	0.000	0.74	0.000								

Notes: The correlation coefficient (*r*) was calculated and the Fisher (*F*) test was conducted to test this linear regression, with its probability (*p*-value) listed. **Bold font** indicates that linear correlation between drought index and FWI is not significant at the 0.05 level (*p*-value > 0.05). The final eight columns are the *r*- and *p*-values calculated in each climate division (CD) for the four drought indices.

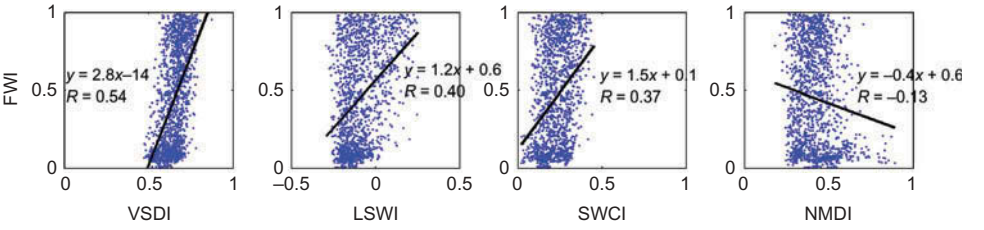

Figure 5. Scatter plots of the four drought indices (VSDI, LSWI, SWCI, and NMDI) and 25 cm FWI with statistics from 49 sites (a total of 1519 samples, 49 sites × 31 periods/site).

From Figure 5, we can see that VSDI presents the strongest correlation with FWI ($r = 0.54$), followed by LSWI ($r = 0.40$) and SWCI ($r = 0.37$), while NMDI was weakest ($r = -0.13$). This infers that VSDI has a better overall capability of drought monitoring compared with other indices. The higher r value of LSWI compared with SWCI can be explained by our site selection, since all sites are located in plant-growing areas, the condition of which is generally more favourable for the application of the vegetation drought index (LSWI) than the SWCI. The weak agreement between NMDI and FWI may be ascribed to the diverse vegetation coverage at each site, which blurs the role of NMDI as a vegetation and soil moisture indicator. In addition, the value range for each index based on the statistics of 49 stations was obtained, which can also be seen from Figure 5: VSDI ranges from 0.47 to 0.9; LSWI ranges from −0.3 to 0.25; SWCI ranges from 0 to 0.45; and NMDI ranges from 0.18 to 0.9. The value range of VSDI is within the ideal range of VSDI between 0 (extremely dry) and 1 (wet) on farmland (Table 1). Given the limited vegetation and soil types covered in this study in Oklahoma, the ideal range of VSDI in Table 1 can be deemed reasonable.

Correlation analysis (Table 2) was also carried out for each site and each CD. The Fisher (F) test was conducted to test this linear regression with its probability (p-value), as listed in Table 2. For each site there were 31 periods during the validation period, and thus 31 samples (one sample per 8 day period); and for each CD, statistics were calculated as CD-specific site number multiplied by 31 periods/site. The bold font indicating linear correlation between drought index and the FWI is not significant at the 0.05 level (p-value > 0.05).

From Table 2, we can see that VSDI, LSWI, and SWCI generally have positive correlations with 25 cm FWI over the 49 sites, while NMDI shows inconsistent correlation with FWI (positive r at some sites and negative at others). Among the 49 stations, VSDI was weakly correlated with FWI (insignificant r) at four sites (HOOK, COPA, MARE, and OKMU), which are located in CD 1, CD 3, CD 5, and CD 6, respectively. The reason for these weak correlations is not very clear and may be partly due to the different phenologic features of the mixed land-cover types (Table 2) at these sites. For example, the pixels of the HOOK site combine grass and idle land, and the COPA site has mixed pixels of grass and forest which have different phenologic stages. Compared with VSDI, more uncertainties exist in the performance of LSWI, SWCI, and NMDI, with insignificant r values shown at 19, 22, and 22 sites, respectively. This comparison demonstrates that VSDI shows more consistency in drought monitoring from site to site in comparison with LSWI and SWCI.

In regard to CD (the final eight columns in Table 2), VSDI shows consistent and strong agreement with FWI variation over all CDs, whereas LSWI and SWCI present a weak correlation with FWI at CD1 and CD6, respectively. In regard to NMDI, although its absolute r value ($|r|$) is significant across all CDs, its instability can still be observed: negative r at

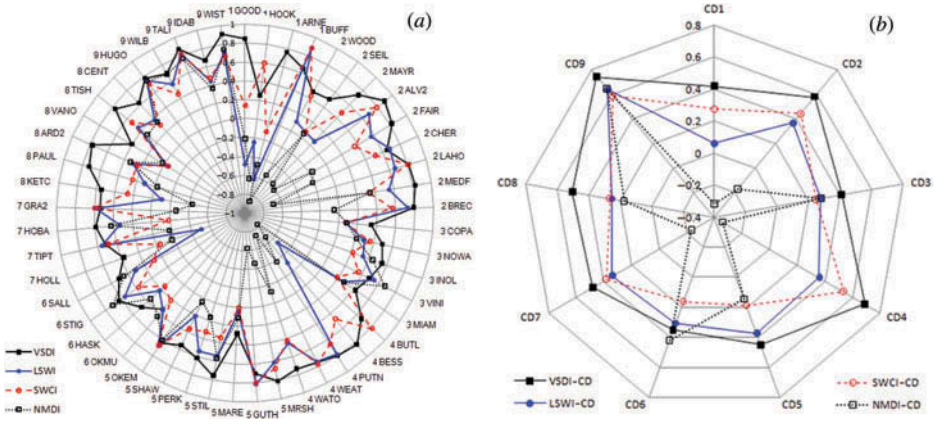

Figure 6. Radar chart of the correlation coefficients (r) between the four drought indices (VSDI, LSWI, SWCI, and NMDI) and FWI over 49 validation sites (plot (a)) and the nine climate divisions (plot (b)).

Notes: The radials represent the r range from -1 to $+1$ for plot (a), and from -0.4 to 0.8 for plot (b). In plot (a), the 49 sites were first clustered by climate division (indicated by the number preceding the station ID) and then ordered in ascending sequence of site longitude. In plot (b), the r for each climate division (CD) was plotted for the four indices indicated by the 'drought index name CD'. In both charts, VSDI r values are concentrated along the outer contour among the four indices, indicating its better performance among sites and climate divisions.

CD 1, CD 2, CD 4, and CD 7 and positive at the remainder. In this sense, VSDI appears to be more operational than the other drought indices over different climate systems.

To obtain an overall image of the performance of the four indices among sites and CDs, the datasets in Table 2 are plotted into two radar charts (Figures 6(a) and (b)). The radials of the radar charts represent the r range from -1 to $+1$ for Figure 6(a) and from -0.4 to $+0.8$ for Figure 6(b).

A similar conclusion can be drawn from Figure 6. As we can see, VSDI r values are concentrated along the outer contour among the four indices in either Figure 6(a) (over 49 sites) or Figure 6(b) (over nine CDs). This demonstrates that VSDI is relatively stable and shows a better performance over diverse sites and diverse climate systems compared with other indices. On the other hand, the higher variability of NMDI r values can also be observed in Figure 6(a) and (b). Therefore, much uncertainty may occur if applying this index from site to site or over different climate systems. Consistent with the findings of a previous study (Shahabfar, Ghulam, and Eitzinger 2012) that the performance of remote sensing drought indices may vary among different climate regions, a close examination of Figure 6(b) also reveals this variation in VSDI. Although VSDI has significant correlation with FWI for all CDs, its r values at CD 1, CD 3, and especially for CD 6, are lower than those for other regions. Two factors may have contributed to this phenomenon. The first is the inclusion of sites having weak correlation with FWI in this CD, such as HOOK in CD 1 and COPA in CD 3. These weak correlations, as we mentioned above, may be partly ascribed to the different phenologic features of mixed land cover. The second reason is that since VSDI does not include thermal bands, it may not perform well in temperature-driven drought areas where precipitation is relatively sufficient and high temperature is the dominant factor in water stress. This may be the case for CD 3 and CD 6, which are characterized by higher precipitation and higher temperatures (Figure 3), and thus high VSDI r values cannot be expected. Overall, the results from Table 2 and Figures 5 and 6 can still verify good agreement between VSDI and soil moisture variation (FWI).

3.2.2. NDVI threshold analysis

To further illustrate the applicability of VSDI to different land-cover types, the NDVI threshold method (Sobrino, Raissouni, and Li 2001; Momeni and Saradjian 2007; Javadnia, Mobasheri, and Kamali 2009) was applied in this study to separate land surface into different types of land cover. Considering that all validation sites were selected in plant-growing areas during the plant-growing season, the land-cover types in this study may not include water or snow water equivalents. Therefore, three land types (Table 3) were finally determined according to the NDVI threshold method: among the total of 1519 samples (49 sites $\times$ 31 periods/site), 32 samples were identified as bare soil (or soil cover) with NDVI < 0.2; 1111 were classified as partially vegetated soil (or mixed cover) with $0.2 \leq$ NDVI ≤ 0.5; and the remaining 376 samples were classified as dense vegetation (or vegetation cover) with NDVI > 0.5. Since plant moisture is not available from Mesonet measurements, the 25 cm FWI was used as an indicator of canopy water at the vegetation cover, assuming that plant moisture has a close relationship with surface soil moisture (Fensholt and Sandholt 2003). The correlation analysis results between the four drought indices and 25 cm FWI over the three land-cover types are presented in Table 3.

From Table 3, we can see that with increase in NDVI, only VSDI displays a gradual reduction in r values, while the other indices show either a sharp decrease (SWCI) or sharp increase (LSWI) or even demonstrate a converse correlation with increase in vegetation coverage (NMDI). For VSDI, its strongest correlation with FWI was observed for soil cover with 0.51, which is slightly lower than that of the soil drought index SWCI (0.67). In regard to mixed cover, VSDI shows a distinct advantage, with a much higher r value (0.45), over other drought indices ($r < 0.2$). For vegetation cover, although VSDI showed the lowest r value (0.42) among the three cover types, it was still the highest among the four indices and even higher than the vegetation drought index LSWI (0.38). The relatively lower correlation of VSDI-FWI for vegetation cover might be explained by the fact that FWI is more indicative of soil moisture than vegetation moisture. Although we can make the assumption above that FWI can be used as an approximation of canopy moisture, this may in fact introduce some uncertainty and might lead to lower correlation with vegetation cover. Nevertheless, the satisfactory overall performance of VSDI represents a unique feature that can be applied over different land-cover types and throughout plant-growing seasons. The vegetation drought index LSWI showed the strongest response to FWI variation for vegetation cover ($r = 0.38$), but showed a weak and inverse correlation with FWI at the soil surface ($r = -0.11$). On the contrary, SWCI, the soil drought index, gave the

Table 3. Correlation coefficient (r) between the four drought indices (VSDI, LSWI, SWCI, and NMDI) and 25 cm FWI for three land-cover types obtained from the NDVI threshold method.

		VSDI		LSWI		SWCI		NMDI	
		r	p-value	r	p-value	R	p-value	r	p-value
Soil cover	NDVI < 0.2 (32 samples)	0.51	0.003	**−0.11**	**0.557**	0.67	0.000	−0.70	0.000
Mixed cover	$0.2 \leq$ NDVI ≤ 0.5 (1111 samples)	0.45	0.000	0.16	0.000	0.18	0.000	−0.14	0.000
Vegetation cover	NDVI > 0.5 (376 samples)	0.42	0.000	0.38	0.000	0.16	0.003	0.40	0.003

Note: A Fisher (F) test was conducted to test this linear regression, and the **bold font** indicates that the linear correlation between drought index and FWI is not significant at the 0.05 level (p-value > 0.05).

highest correlation with FWI for soil cover ($r = 0.67$) but the lowest correlation for vegetation cover ($r = 0.16$). These phenomena are quite reasonable: since LSWI was designed as a vegetation moisture indicator, its best performance can be expected for dense vegetation, while for SWCI, the role of which is as a soil moisture indicator, its best performance is expected for bare soil surfaces. In regard to NMDI, its correlation with FWI varied among different land-cover types, with a positive r for vegetation cover and negative r for bare soil and mixed cover.

In summary, the results from Table 3 verify the wide applicability of VSDI over different land-cover types, and at the same time reveal the restricted applicability of other drought indices. LSWI (the vegetation drought index) is more efficient for dense vegetation than for a sparsely vegetated or bare soil surface, and SWCI (the soil drought index) works well at the soil surface but not for vegetation cover. NMDI, although originally designed for both soil and vegetation surfaces, is not suitable for drought monitoring over a large area or during plant-growing seasons, due to its inconsistent relationship with moisture variation among different land-cover types.

3.2.2. Time-lag analysis

Time-lag analysis is also conducted in this study to examine the promptness of drought warning for the four drought indices. Correlation coefficients (r) with a time lag from 0 periods (no time lag) to 5 periods (40 day lag) for each index over the nine CDs are presented in Figure 7. The dotted line indicates the significant threshold at the 95% confidence level with a 5 period lag for each CD.

It is easy to see from Figure 7 that VSDI presents the highest correlation with FWI in the study period over nine CDs. This indicates that either no time lag exists between VSDI and 25 cm FWI or the time lag of VSDI is less than 8 days. In this sense, VSDI can be viewed as a real-time drought indicator. In regard to SWCI, its time-lag pattern is similar to that of VSDI, with no time lag over nine CDs except for CD 7, where a 2–3 period lag can be observed. In contrast, the time lag for LSWI is more prominent, and different lag periods can be observed at different CDs. For example, the time lag of LSWI seems to be more than 5 periods in CD 1, CD 5, and CD 6, about 1–3 periods in CD 3, CD 7, CD 8, and CD 9, and its time lag is unperceivable at CD 2 and CD 4. In regard to NMDI, it generally showed higher correlation during the study period with FWI, with two exceptions at CD 2 and CD 8, where lags of 5 and 3 periods were observed, respectively. In general, compared with LSWI, SWCI, and NMDI, VSDI is more like a real-time drought indicator with a time lag to 25 cm soil moisture of less than 8 days.

3.3. Comparison with USDM

One important function of the drought index is to quantify drought severity for the area concerned. In this case, the VSDI drought maps of Oklahoma were produced and compared with USDM maps. The USDM map is a weekly drought product developed by a partnership of various agencies including NOAA, the US Department of Agriculture (USDA), and the National Drought Mitigation Center (NDMC) (http://www.drought.unl.edu/MonitoringTools/USDroughtMonitor.aspx). It combines multiple indicators, including the Palmer drought index, the standardized precipitation index (SPI), soil moisture percentiles from the Climate Prediction Center (CPC), USGS weekly streamflow percentiles, and professional input from all levels to provide a 'big picture' assessment of drought conditions across the USA (Svoboda et al. 2002). USDM archive maps are available at http://droughtmonitor.unl.edu/archive.html

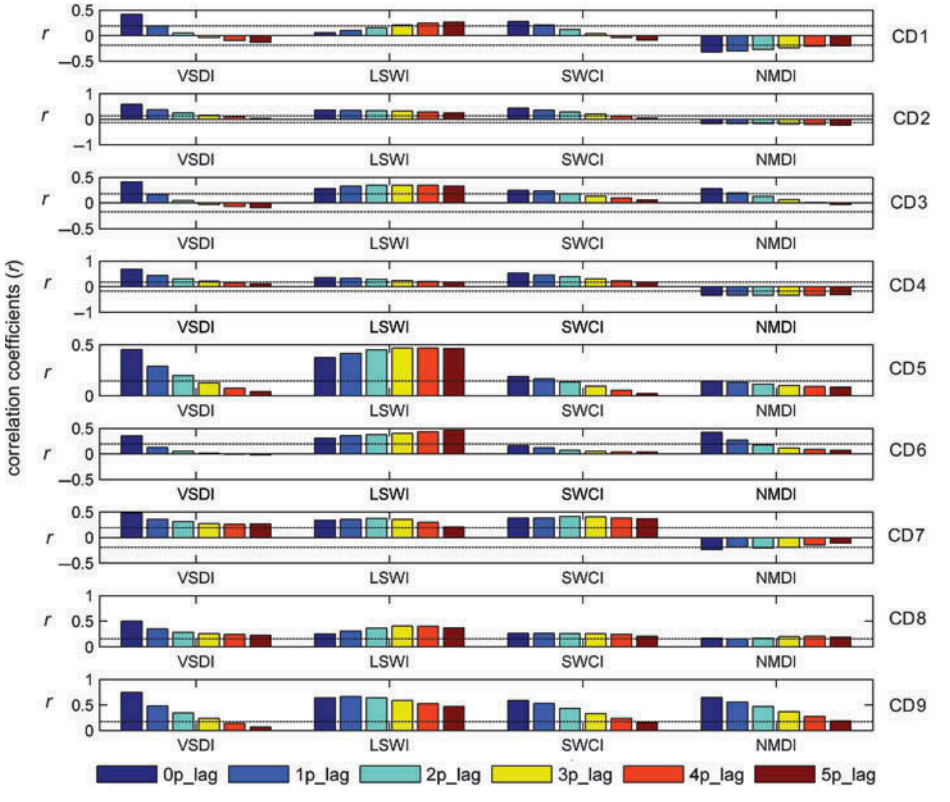

Figure 7. Correlation coefficients (r) between the four drought indices (VSDI, LSWI, SWCI, and NMDI) and 25 cm FWI with time lag from 0 periods (0p lag, no time lag) to 5 periods (5p lag, 40 day lag) over nine climate divisions.

Note: The dotted line indicates the significant threshold at the 95% confidence level with a 5 period lag for each climate division.

The first step to producing a VSDI drought map is to identify the drought severity classes. To be comparable with USDM, six classes were determined according to the drought categories of USDM: Normal, Abnormally Dry, Moderate Drought, Severe Drought, Extreme Drought, and Exceptional Drought, by cross-referring to FWI (Table 4). According to Illston, Basara, and Crawford (2004), 'the majority of vegetation across Oklahoma will flourish when FWI values are greater than 0.8. The vegetation will strain and wilt from diminished moisture when FWI values are approximately 0.5, and begin to die when FWI values are 0.3 or less'. Therefore, 0.7, 0.6, 0.5, 0.4, and 0.3 were selected as the five FWI thresholds to classify drought status into the six classes. FWI thresholds were then taken as the dependent variable (y) into a linear regression equation between 25 cm FWI and VSDI based on statistics from all sites (Figure 5, $y = 2.8 \times \mathrm{x} - 1.4$; $r = 0.54$); in this way the thresholds of VSDI (listed in Table 4) can be determined.

Since USDM is updated weekly while VSDI was calculated based on the 8 day MODIS product, there is a slight difference in time-stamp between the two maps. During our validation period (6 March to 8 November), there were 5 days that matched between VSDI and USDM maps (29 March, 24 May, 19 July, 13 September, and 8 November), and these are plotted in Figure 8.

As we can see from Figure 8, overall agreement can be recognized between VSDI and USDM maps with similar drought patterns between the two products. The onset of drought

Table 4. Drought classification scheme of FWI and VSDI.

Drought type	FWI range	VSDI range
Normal	FWI $\geq$ 0.7	VSDI $\geq$ 0.75
D0, Abnormally dry	0.6 $\leq$ FWI $<$ 0.7	0.71 $\leq$ VSDI $<$ 0.75
D1, Moderate drought	0.5 $\leq$ FWI $<$ 0.6	0.68 $\leq$ VSDI $<$ 0.71
D2, Severe drought	0.4 $\leq$ FWI $<$ 0.5	0.64 $\leq$ VSDI $<$ 0.68
D3, Extreme drought	0.3 $\leq$ FWI $<$ 0.4	0.61 $\leq$ VSDI $<$ 0.64
D4, Exceptional drought	FWI $<$ 0.3	VSDI $<$ 0.61

in Oklahoma was observed in March and May, the severe drought prevalent throughout Oklahoma was captured in July and September, and a relatively improved drought status can also be perceived for November. In addition, VSDI shows a more detailed spatial variation of drought conditions within each county of Oklahoma, whereas USDM presents a relatively rough picture at the county level with several counties classified at the same drought level. This may be credited as one advantage of the VSDI drought map over USDM, considering the USDM map is not designed to depict local conditions (see USDM official website, http://droughtmonitor.unl.edu/classify.htm).

However, there are also certain differences between the two products. First, an obvious linear segmentation can be observed in the VSDI map on 29 March in east Oklahoma. This segmentation was mainly caused by the image mosaic in data preprocessing. Besides, on 8 November, the Oklahoma drought condition on the VSDI map seems less severe than that on USDM maps. To explain this phenomenon, the drought summaries for that week reported by Brian Fuchs from the National Drought Mitigation Center from the USDM website (http://droughtmonitor.unl.edu/archive.html) are cited below.

A series of rain events over the last week, with the latest coming at the end of the current US Drought Monitor period, allowed for improvements over Oklahoma and into the extreme northern counties of Texas Improvements were made in eastern and central Oklahoma, where a categorical improvement was made over areas receiving the bulk of the precipitation.

Thus the overall improved drought status on the VSDI map can be attributed to the precipitation that week, especially for eastern and central Oklahoma, which are indicated as normal or abnormally dry on the VSDI map. Since VSDI is a single moisture indicator, it may have a more direct and rapid response to precipitation than the multi-indicator combined USDM product (e.g. the former includes several climatologically based indicators), which still shows a lingering drought over Oklahoma. The VSDI classification scheme can also contribute to subtle differences between VSDI and USDM maps. For reference, the VSDI thresholds in this study were readily calculated from linear regression using empirically defined FWI thresholds. A specific set of thresholds for other regions or other methods could be explored for drought classification in a future study.

4. Summary and conclusion

In this article, a simple but effective method for agricultural drought monitoring, the VSDI, was developed. This index was designed by exploiting the difference between moisture-sensitive bands (SWIR and red) and a moisture reference band (blue), and is expected to complement the scarcity of agricultural drought monitoring over different land-cover types and through the plant-growing season. The validation of VSDI was carried out in Oklahoma

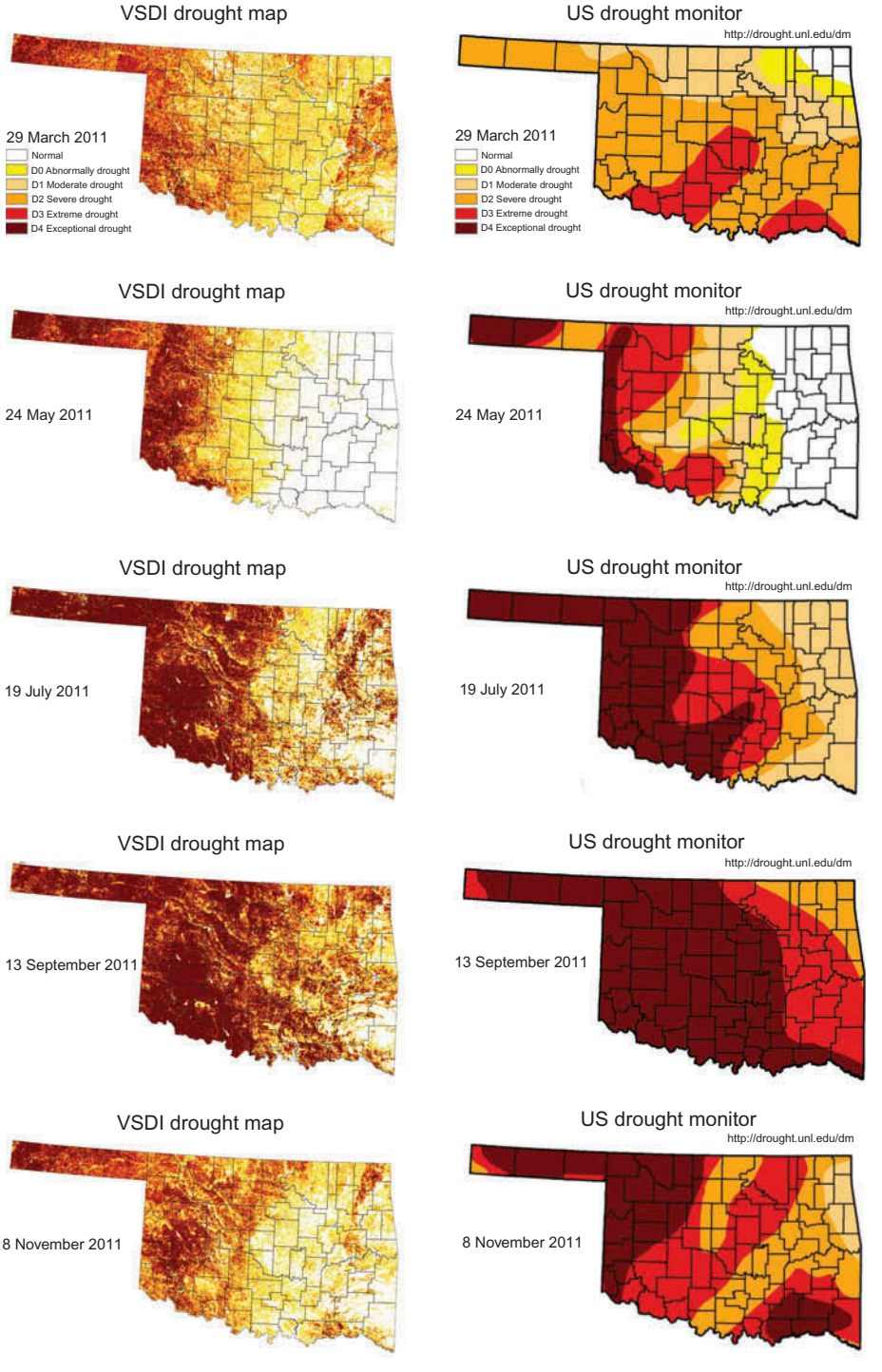

Figure 8. Five matched dates between VSDI 8 day drought maps and USDM weekly maps of Oklahoma on 29 March, 24 May, 19 July, 13 September, and 8 November.

Note: VSDI maps showed overall good agreement with USDM results, and can reveal finer spatial variation of drought than USDM.

using soil moisture measurements from 49 Mesonet stations. The correlation coefficient between VSDI and 25 cm soil moisture (FWI) was calculated and compared with LSWI, SWCI, and NMDI over 49 sites and nine CDs. The NDVI threshold method was applied to examine the applicability of VSDI and three other indices over different land-cover types. Time-lag analysis was also conducted over nine CDs to evaluate the time response to moisture variation for the four drought indices. Finally, a drought classification scheme based on VSDI is suggested in this article, and the VSDI drought maps were produced and compared with USDM maps. Based on the above analysis, we came to the following conclusions.

(1) Taking advantage of multi-spectral information, VSDI has a clear biophysical connotation and consistently characterizes well the moisture dynamics over both soil and vegetation surfaces. Compared with LSWI, SWCI, and NMDI, VSDI presented the strongest correlation with 25 cm FWI over 49 stations and nine climate systems throughout the plant-growing season.
(2) The NDVI threshold method reveals that VSDI is applicable over different land-cover types. This is a major advantage over the current optical drought indices, since LSWI (the vegetation moisture index) performs best for vegetation surfaces, while SWCI is efficient only for bare soil cover, and NMDI, which was originally designed to monitor both soil and vegetation moisture, has an inconsistent correlation with moisture variation for different land surfaces.
(3) Time-lag analysis over nine CDs in Oklahoma indicated that VSDI has no time lag (or its time lag is within 8 days) in response to soil moisture variation in Oklahoma. Other indices displayed greater or less time lag according to CD. Therefore, VSDI may be used as a real-time drought indicator and in future work other study areas should be considered to further validate this feature.
(4) The good agreement between VSDI drought maps and USDM maps indicates the favourable performance of VSDI in drought monitoring. VSDI maps display finer spatial variation of drought conditions compared with USDM products, and VSDI may be applied for drought monitoring at both the regional scale and above.
(5) The main limitation of VSDI is that it was developed using only optical spectral bands and does not take into account temperature information, which is an important factor in drought development. Therefore, this index may not perform well in drought-prone areas where temperature is the major constraint rather than precipitation. This point is briefly discussed in this article. In our future work, other study areas will be included to validate the performance of VSDI over different climate systems, and the thermal band may be introduced to VSDI to enhance its ability in drought monitoring and warning.
(6) Further work is still required to evaluate the performance of VSDI. The following issues will be considered and addressed in our follow-up work: (1) discussion of point-to-point variability in *in situ* soil moisture (or FWI) and how it affects FWI–VSDI correlation; (2) evaluation of VSDI from the viewpoint of meteorological drought by comparing it with meteorological data and drought indices (such as precipitation measurements, SPI, or *z*-score index); and (3) incorporation of soil and vegetation type in the analysis of the time-lag effect of VSDI and other drought indices.

Acknowledgements

The authors would like to thank the Mesonet network (http://www.mesonet.org) for providing the ground measurement data. The MODIS reflectance products (MOD09A1) used in this study were collected from http://ladsweb.nascom.nasa.gov/data The CDL used in this study was downloaded from the Geospatial Data Gateway at http://datagateway.nrcs.usda.gov/. The archive maps of the USDM were obtained from http://droughtmonitor.unl.edu/archive.html The authors also thank anonymous reviewers for their critical and helpful comments and suggestions. The authors appreciate the generous financial support of the National Natural Science Foundation of China (No. 41071221, No. 41201331) and the R&D Special Fund for Public Welfare Industry of China (Meteorology) (No. GYHY 200806022). The lead author would also like to thank the HyDROS Lab (http://hydro.ou.edu) at the National Weather Center, Norman, Oklahoma.

References

Adegoke, J. O., and A. M. Carleton. 2002. "Relations Between Soil Moisture and Satellite Vegetation Indices in the U.S. Corn Belt." *Journal of Hydrometeorology* 3: 395–405.

Aldakheel, Y. Y., and F. M. Danson. 1997. "Spectral Reflectance of Dehydrating Leaves: Measurements and Modeling." *International Journal of Remote Sensing* 18: 3683–3690.

Anyamba, A., C. J. Tucker, and J. R. Eastman. 2001. "NDVI Anomaly Patterns Over Africa During the 1997/98 ENSO Warm Event." *International Journal of Remote Sensing* 22: 1847–1859.

Bach, H., and W. Verhoef. 2003. "Sensitivity Studies on the Effect of Surface Soil Moisture on Canopy Reflectance Using the Radiative Transfer Model GeoSAIL." In *Geoscience and Remote Sensing Symposium, IGARSS '03*, 1679–1681. IEEE International. doi: 10.1109/IGARSS.2003.1294215.

Baumgardner, M. F., L. F. Silva, L. L. Biehl, and E. R. Stoner. 1985. "Reflectance Properties of Soils." *Advances in Agronomy* 38: 1–44.

Bowers, S. A., and R. J. Hanks. 1965. "Reflectance of Radiant Energy from Soils." *Soil Science* 100: 130–138.

Brock, F. V., K. C. Crawford, R. L. Elliott, G. W. Cuperus, S. J. Stadler, H. L. Johnson, and M. D. Eilts. 1995. "The Oklahoma Mesonet: A Technical Overview." *Journal of Atmospheric and Oceanic Technology* 12: 5–19.

Brown, J. F., B. D. Wardlow, T. Tadesse, M. J. Hayes, and B. C. Reed. 2008. "The Vegetation Drought Response Index (VegDRI): A New Integrated Approach for Monitoring Drought Stress in Vegetation." *GIScience Remote Sensing* 45: 16–46. doi:10.2747/1548-1603.45.1.16.

Carter, A. C. 1991. "Primary and Secondary Effects of Water Content on the Spectral Reflectance of Leaves." *American Journal of Botany* 78: 916–924.

Carter, A. C. 1993. "Responses of Leaf Spectral Reflectance to Plant Stress." *American Journal of Botany* 80: 239–243.

Ceccato, P., S. Flasse, S. Tarantola, S. Jacquemoud, and J. Gregoire. 2001. "Detecting Vegetation Leaf Water Content Using Reflectance in the Optical Domain." *Remote Sensing of Environment* 77: 22–33.

Ceccato, P., N. Gobron, S. Flasse, B. Pinty, and S. Tarantola. 2002. "Designing a Spectral Index to Estimate Vegetation Water Content from Remote Sensing Data: Part 1 Theoretical Approach." *Remote Sensing of Environment* 82: 188–197.

Chen, D., J. Huang, and T. J. Jackson. 2005. "Vegetation Water Content Estimation for Corn and Soybeans Using Spectral Indices Derived from Modis Near- and Short-Wave Infrared Bands." *Remote Sensing of Environment* 98: 225–236.

Chen, W., Q. Xiao, and Y. Sheng. 1994. "Application of the Anomaly Vegetation Index to Monitoring Heavy Drought in 1992." *Remote Sensing of Environment* 9: 106–112. (in Chinese).

Chuvieco, E., D. Riãno, I. Aguado, and D. Cocero. 2002. "Estimation of Fuel Moisture Content from Multitemporal Analysis of Landsat Thematic Mapper Reflectance Data: Applications in Fire Danger Assessment." *International Journal of Remote Sensing* 23: 2145–2162.

Dawson, T. P., P. J. Curran, P. R. J. North, and S. E. Plummer. 1999. "The Propagation of Foliar Biochemical Absorption Features in Forest Canopy Reflectance: A Theoretical Analysis." *Remote Sensing of Environment* 67: 147–159.

Di, L., D. C. Rundquist, and L. Han. 1994. "Modelling Relationships Between NDVI and Precipitation During Vegetative Growth Cycles." *International Journal Remote Sensing* 15: 2121–2136.

Dracup, J. A., K. S. Lee, and E. G. J. Paulson. 1980. "On the Definition of Drought." *Water Resources Research* 16: 297–302.

Du, X., S. Wang, Y. Zhou, and H. Wei. 2007. "Construction and Validation of a New Model for Unified Surface Water Capacity Based on MODIS Data." *Geomatics and Information Science of Wuhan University* 32: 205–207. (in Chinese).

Elachi, C.1987. *Introduction to the Physics and Techniques of Remote Sensing*, 66–71. New York: John Wiley.

Elvidge, C. D. 1990. "Visible and Infrared Reflectance Characteristics of Dry Plant Materials." *International Journal of Remote Sensing* 11: 1775–1795.

Elvidge, C. D., and R. J. P. Lyon. 1985. "Estimation of the Vegetation Contribution to the 1.65/2.22 μm Ratio in Airborne Thematic-Mapper Imagery of the Virginia Range, Nevada." *International Journal of Remote Sensing* 6: 75–88.

FEMA. 1995. "National Mitigation Strategy: Partnerships for Building Safer Communities." *FEMA Mitigation Directorate*, 40 p.

Fensholt, R., and I. Sandholt. 2003. "Derivation of a Shortwave Infrared Stress Index from MODIS Near- and Shortwave Infrared Data in a Semiarid Environment." *Remote Sensing of Environment* 87: 111−121.

Gao, B. C. 1996. "NDWI—A Normalized Difference Water Index for Remote Sensing of Vegetation Liquid Water from Space." *Remote Sensing of Environment* 58: 257–266.

Ghulam, A., T. M. Kusky, T. Teyip, and Q. Qin. 2011. "Sub-Canopy Soil Moisture Modeling in n-Dimensional Spectral Feature Space." *Photogrammetric Engineering and Remote Sensing* 77: 149–156.

Ghulam, A., Z. Li, Q. Qin, Q. Tong, J. Wang, A. Kasimu, and L. Zhu. 2007a. "A Method for Canopy Water Content Estimation for Highly Vegetated Surfaces-Shortwave Infrared Perpendicular Water Stress Index." *Science in China Series D: Earth Sciences* 50: 957–965.

Ghulam, A., Z. Li, Q. Qin, H. Yimit, and J. Wang. 2008a. "Estimating Crop Water Stress with ETM+ NIR and SWIR Data." *Agricultural and Forest Meteorology* 148: 1679–1695.

Ghulam, A., Q. Qin, T. Kuskya, and Z. Li. 2008b. "A Re-Examination of Perpendicular Drought Indices." *International Journal of Remote Sensing* 29: 6037–6044. doi:10.1080/01431160802235811.

Ghulam, A., Q. Qin, T. Teyip, and Z. Li. 2007b. "Modified Perpendicular Drought Index (MPDI): A Real-Time Drought Monitoring Method." *ISPRS Journal of Photogrammetry & Remote Sensing* 62: 150–164.

Ghulam, A., Q. Qin, and Z. Zhan. 2006. "Designing of the Perpendicular Drought Index." *Environmental Geology* 52: 1045–1052.

Gorry, P. A. 1990. "General Least-Squares Smoothing and Differentiation by the Convolution (Savitzky–Golay) Method." *Analytical Chemistry* 62: 570–573.

Gu, Y., J. F. Brown, J. P. Verdin, and B. Wardlow. 2007. "A Five-Year Analysis of MODIS NDVI and NDWI for Grassland Drought Assessment Over the Central Great Plains of the United States." *Geophysical Research Letters* 34: L06407.

Gu, Y., E. Hunt, B. Wardlow, J. B. Basara, J. F. Brown, and J. P. Verdin. 2008. "Evaluation of MODIS NDVI and NDWI for Vegetation Drought Monitoring Using Oklahoma Mesonet Soil Moisture Data." *Geophysical Research Letters* 35: L22401.

Gutman, G.1990. "Towards Monitoring Droughts from Space." *Journal of Climate* 2: 282–295.

Hardisky, M. A., V. Klemas, and R. M. Smart. 1983. "The Influences of Soil Salinity, Growth form, and Leaf Moisture on the Spectral Reflectance of Spartina Alterniflora Canopies." *Photogrammetric Engineering and Remote Sensing* 49: 77–83.

Heim, R. R. 2002. "A Review of Twentieth-Century Drought Indices Used in the United States." *Bulletin of the American Meteorological Society* 83: 1149–1165.

Hunt, E. R. Jr, and B. N. Rock. 1989. "Detection of Changes in Leaf Water Content Using Near and Middle–Infrared Reflectances." *Remote Sensing of Environment* 30: 43–54.

Hunt, E. R. Jr, B. N. Rock, and P. S. Nobel. 1987. "Measurement of Leaf Relative Water Content by Infrared Reflectance." *Remote Sensing of Environment* 22: 429–435.

Illston, B. G., J. B. Basara, and K. C. Crawford. 2004. "Seasonal to Interannual Variations of Soil Moisture Measured in Oklahoma." *International Journal of Climatology* 24: 1883–1896.

Jackson, T. J., D. Chen, M. Cosh, F. Li, M. Anderson, C. Walthall, P. Doriaswamy, and E. R. Hunt. 2004. "Vegetation Water Content Mapping Using Landsat Data Derived Normalized Difference Water Index for Corn and Soybeans." *Remote Sensing of Environment* 92: 475–482.

Jackson, R. D., P. N. Slater, and P. J. Pinter Jr. 1983. "Discrimination of Growth and Water Stress in Wheat by Various Vegetation Indices Through Clear and Turbid Atmospheres." *Remote Sensing of Environment* 13: 187–208.

Jacquemoud, S. 1993. "Inversion of the PROSPECT + SAIL Canopy Reflectance Model from AVIRIS Equivalent Spectra: Theoretical Study." *Remote Sensing of Environment* 44: 281–292.

Jacquemoud, S., and F. Baret. 1990. "PROSPECT: A Model of Leaf Optical Properties Spectra." *Remote Sensing of Environment* 34: 75–91.

Jacquemoud, S., F. Baret, B. Andrieu, F. M. Danson, and K. W. Jaggard. 1995. "Extraction of Vegetation Biophysical Parameters by Inversion of the PROSPECT-SAIL Models on Sugar Beet Canopy Reflectance Data. Application to TM and AVIRIS Sensors." *Remote Sensing of Environment* 52: 163–172.

Javadnia, E., M. R. Mobasheri, and G. A. Kamali. 2009. "MODIS NDVI Quality Enhancement Using ASTER Images." *Journal of Agricultural Science and Technology* 11: 549–558.

Jensen, J. R. 2007. *Remote Sensing of the Environment: An Earth Resource Perspective*. 2nd ed. Upper Saddle River, NJ: Prentice Hall.

Ji, L., and A. J. Peters. 2003. "Assessing Vegetation Response to Drought in the Northern Great Plains Using Vegetation and Drought Indices." *Remote Sensing of Environment* 87: 85–98.

Johnson, D. M., and R. Mueller. 2010. "The 2009 Cropland Data Layer." *Photogrammetric Engineering and Remote Sensing* 1202–1205. Accessed March 12, 2013. http://www.nass.usda.gov/research/Cropland/docs/JohnsonPE&RS_Nov2010.pdf

Kogan, F. N. 1990. "Remote Sensing of Weather Impacts on Vegetation in non-homogenous areas." *International Journal Remote Sensing* 11: 1405–1419.

Kogan, F. N. 1995. "Application of Vegetation Index and Brightness Temperature for Drought Detection." *Advances in Space Research* 15: 91–100.

Kogan, F. N. 1997. "Global Drought Watch from Space." *Bulletin of the American Meteorological Society* 78: 621–636.

Kogan, F. N. 2000. "Contribution of Remote Sensing to Drought Early Warning. In *Early Warning Systems for Drought Preparedness and Drought Management*. Proceedings of the Expert Group Meeting, edited by D. A. Wilhite, M. V. K. Sivakumar, and D. A. Wood, Lisbon. World Meteorological Organization, 86–100. Accessed March 12, 2013. http://www.wamis.org/agm/pubs/agm2/agm02.pdf

Lillesand, T., R. W. Kiefer, and J. W. Chipman. 2008. *Remote Sensing and Image Interpretation*. 6th ed. 1–60. New York: John Wiley & Sons.

Liu, W., F. Baret, X. Gu, Q. Tong, L. Zheng, and B. Zhang. 2002. "Relating Soil Surface Moisture to Reflectance." *Remote Sensing of Environment* 81: 238–246.

Liu, W., F. Baret, X. Gu, B. Zhang, Q. Tong, and L. Zheng. 2003. "Evaluation of Methods for Soil Surface Moisture Estimation from Reflectance Data." *International Journal of Remote Sensing* 24: 2069–2083.

Lobell, D. B., and G. P. Asner. 2002. "Moisture Effects on Soil Reflectance." *Soil Science Society of America Journal* 66(3): 722–27. doi: 10.2136/sssaj2002.7220.

Maki, M., M. Ishiahra, and M. Tamura. 2004. "Estimation of Leaf Water Status to Monitor the Risk of Forest Fires by Using Remotely Sensed Imagery." *Remote Sensing of Environment* 90: 441–450.

McVicar, T. R., and P. N. Bierwirth. 2001. "Rapidly Assessing the 1997 Drought in Papua New Guinea Using Composite AVHRR Imagery." *International Journal Remote Sensing* 22: 2109–2128.

McVicar, T. R., and D. L. B. Jupp. 1998. "The Current and Potential Operational Uses of Remote Sensing to Aid Decisions on Drought Exceptional Circumstances in Australia: A Review." *Agriculture System* 57: 399–468.

Mishra, A. K., and V. P. Singh. 2010. "A Review of Drought Concepts." *Journal of Hydrology* 391: 202–216.

Momeni, M., and M. R. Saradjian. 2007. "Evaluating NDVI-Based Emissivities of MODIS Bands 31 and 32 Using Emissivities Derived by Day/Night LST Algorithm." *Remote Sensing of Environment* 106: 190–198.

Niemeyer, S. 2008. "New Drought Indices." *Options Méditerranéennes, Series A* 80: 267–274.

Ollinger, S. V. 2011. "Sources of Variability in Canopy Reflectance and the Convergent Properties of Plants." *New Phytologist* 189: 375–394. doi:10.1111/j.1469-8137.2010.03536.x.

Phillips, D. 2002. "The Top Ten Canadian Weather Stories for 2001." *CMOS Bull* 30: 19–23.

Qin, Q., A. Ghulam, L. Zhu, L. Wang, J. Li, and P. Nan. 2008. "Evaluation of MODIS Derived Perpendicular Drought Index for Estimation of Surface Dryness Over Northwestern China." *International Journal of Remote Sensing* 29: 1983–1995. doi:10.1080/01431160701355264.

Qin, Q., C. Jin, N. Zhang, and X. Yang. 2010. "An Two-Dimensional Spectral Space Based Model for Drought Monitoring and Its Re-Examination." *International Geoscience and Remote Sensing Symposium (IGARSS 2010)* 3869–3872. doi: 10.1109/IGARSS.2010.5649710.

Ripple, W. J. 1986. "Spectral Reflectance Relationships to Leaf Water Stress." *Environmental Sciences* 52: 1669–1675.

Roberts, D. A., R. O. Green, and J. B. Adams. 1997. "Temporal and Spatial Patterns in Vegetation and Atmospheric Properties from AVIRIS." *Remote Sensing of Environment* 62: 223–240.

Savitzky, A., and M. J. E. Golay. 1964. "Smoothing and Differentiation of Data by Simplified Least-Squares Procedures." *Analytical Chemistry* 36: 1627–1639.

Schneider, J. M., D. K. Fisher, R. L. Elliott, G. O. Brown, and C. P. Bahrmann. 2003. "Spatiotemporal Variations in Soil Water: First Results from the ARM SGP CART Network." *Journal of Hydrometeorology* 4: 106–120.

Shahabfar, A., A. Ghulam, and J. Eitzinger. 2012. "Drought Monitoring in Iran Using the Perpendicular Drought Indices." *International Journal of Applied Earth Observation and Geoinformation* 18: 119–127.

Sims, D. A., and J. A. Gamon. 2003. "Estimation of Vegetation Water Content and Photosynthetic Tissue Area from Spectral Reflectance: A Comparison of Indices Based on Liquid Water and Chlorophyll Absorption Features." *Remote Sensing of Environment* 84: 526–537.

Sobrino, J. A., N. Raissouni, and Z. Li. 2001. "A Comparative Study of Land Surface Emissivity Retrieval from NOAA Data." *Remote Sensing of Environment* 75: 256–266.

Svoboda, M., D. LeComte, M. Hayes, R. Heim, K. Gleason, J. Angel, B. Rippey, R. Tinker, M. Palecki, D. Stooksbury, D. Miskus, and S. Stephens. 2002. "The Drought Monitor." *Bulletin of the American Meteorological Society* 83: 1181–1190.

Tucker, C. J. 1980. "Remote Sensing of Leaf Water Content in the Near-Infrared." *Remote Sensing of Environment* 10: 23–32.

Wan, Z., P. Wang, and X. Li. 2004. "Using MODIS Land Surface Temperature and Normalized Difference Vegetation Index for Monitoring Drought in the Southern Great Plains, USA." *International Journal of Remote Sensing* 25: 61–72.

Wang, J., K. P. Price, and P. M. Rich. 2001. "Spatial Patterns of NDVI in Response to Precipitation and Temperature in the Central Great Plains." *International Journal Remote Sensing* 22: 3827–3844.

Wang, L., and J. J. Qu. 2007. "NMDI: A Normalized Multi-Band Drought Index for Monitoring Soil and Vegetation Moisture with Satellite Remote Sensing." *Geophysical Research Letters* 34: L20405. doi:10.1029/2007GL031021.

Wang, L., and J. J. Qu. 2009. "Satellite Remote Sensing Applications for Surface Soil Moisture Monitoring: A Review." *Frontiers of Earth Science in China* 3: 237–247.

Wang, X., H. Xie, H. Guan, and X. Zhou. 2007. "Different Responses of MODIS-Derived NDVI to Root-Zone Soil Moisture in Semi-Arid and Humid Regions." *Journal of Hydrology* 340: 12–24.

Wardlow, B. D., M. C. Anderson, and J. P. Verdin. 2012. *Remote Sensing of Drought: Innovative Monitoring Approaches*. Boca Raton, FL: CRC Press.

Wheaton, E. E., L. M. Arthur, B. Chorney, C. Shewchuk, J. Thorpe, J. Whitting, and K. Whittrock. 1992. "The Prairie Drought of 1988." *Climatological Bulletin* 26: 188–205.

Whiting, M. L., L. Li, and S. L.Ustin. 2004. "Predicting Water Content Using Gaussian Model on Soil Spectra." *Remote Sensing of Environment* 89: 535–552.

Wilhite, D. A., ed. 2000. "Drought as a Natural Hazard: Concepts and Definitions." In *Drought Volume I: A Global Assessment*, 3–18. New York: Routledge.

Xiao, X., D. Hollinger, J. Aber, M. Goltz, E. A. Davidson, Q. Zhang, and B. Moore III. 2004a. "Satellite-Based Modeling of Gross Primary Production in an Evergreen Needleleaf Forest." *Remote Sensing of Environment* 89: 519–534.

Xiao, X., Q. Zhang, B. Braswell, S. Urbanski, S. Boles, S. C. Wofsy, B. Moore III, and D. Ojima. 2004b. "Modeling Gross Primary Production of Temperate Deciduous Broadleaf Forest Using Satellite Images and Climate Data." *Remote Sensing of Environment* 91: 256–270.

Yang, N., Q. Qin, C. Jin, and Y. Yao. 2008. "The Comparison and Application of the Methods for Monitoring Farmland Drought Based on NIR-Red Spectral Space." *International Geoscience and Remote Sensing Symposium (IGARSS 2008)* III871–III874. doi: 10.1109/IGARSS.2008.4779488.

Yu, G., T. Miwa, K. Nakayama, N. Matsuoka, and H. Kon. 2000. "A Proposal for Universal Formulas for Estimating Leaf Water Status of Herbaceous and Woody Plants Based on Spectral Reflectance Properties." *Plant Soil* 227: 47–58.

Zarco-Tejada, P. J., C. A. Rueda, and S. L. Ustin. 2003. "Water Content Estimation in Vegetation with MODIS Reflectance Data and Model Inversion Methods." *Remote Sensing of Environment* 85: 109–124.

Zhang, H., H. Chen, S. Shen, G. Zhou, and W. Yu. 2008. "Drought Remote Sensing Monitoring Based on the Surface Water Content Index (SWCI) Method." *Remote Sensing Technology and Application* 23: 624–628. (in Chinese)

Zhang, J., Y. Xu, F. Yao, P. Wang, W. Guo, L. Li, and L. Yang. 2010. "Advances in Estimation Methods of Vegetation Water Content Based on Optical Remote Sensing Techniques." *Science China-Technological Sciences* 53: 1159–1167.

Zhao, S., Q. Qin, L. You, Y. Yao, N. Yang, and J. Li. 2009. "Application of Two Shortwave Infrared Water Stress Indices to Drought Monitoring Over Northwestern China." *Geoscience and Remote Sensing Symposium(IGARSS 2009)* III-530–III-533. doi: 10.1109/IGARSS.2009.5417809.

Zygielbaum, A. I., A. A. Gitelson, T. J. Arkebauer, and D. C. Rundquist. 2009. "Non-Destructive Detection of Water Stress and Estimation of Relative Water Content in Maize." *Geophysical Research Letters* 36: L12403.